

# Switched forced SEIRDV compartmental models to monitor COVID-19 spread and immunization in Italy

Erminia Antonelli

Department of Mathematics, University of Bologna, ITALY (e-mail: [erminia.antonelli@studio.unibo.it](mailto:erminia.antonelli@studio.unibo.it))

Elena Loli Piccolomini

Department of Computer Science and Engineering, University of Bologna, ITALY (e-mail:

[elena.loli@unibo.it](mailto:elena.loli@unibo.it))

Fabiana Zama

Department of Mathematics, University of Bologna, ITALY (e-mail: [fabiana.zama@unibo.it](mailto:fabiana.zama@unibo.it))

---

## Abstract

This paper presents a new hybrid compartmental model for studying the COVID-19 epidemic evolution in Italy since the beginning of the vaccination campaign started on 2020/12/27 and shows forecasts of the epidemic evolution in Italy. The proposed compartmental model subdivides the population into six compartments and extends the SEIRD model proposed in [E.L.Piccolomini and F.Zama, PLOS ONE, 15(8):1–17, 08 2020] by adding the Vaccinated population and framing the global model as a hybrid-switched dynamical system. Aiming to represent the quantities that characterize the epidemic behaviour from an accurate fit to the observed data, we partition the observation time interval into sub-intervals. The model parameters change according to a switching rule depending on the data behaviour and the infection rate continuity condition. In particular, we study the representation of the infection rate both as linear and exponential piecewise continuous functions. We choose the length of sub-intervals balancing the data fit with the model complexity through the Bayesian Information Criterion. The calibration of the model shows an excellent representation of the epidemic behaviour and thirty days forecasts have proven to reproduce the infection spread reliably. Finally, we discuss different possible forecast scenarios obtained by simulating an increased vaccination rate.

*Keywords:* Compartmental model with Vaccine, SEIRDV, switched model, hybrid model, forcing function, model calibration.

---

## 1. Introduction

Compartmental models are essential mathematical tools in the analysis of the evolution of epidemics, for prediction and simulation of future strategies which can be used by governments and policymakers to allocate sanitary and economic resources. The parameters of such models are related to meaningful characteristics of the epidemic disease, such as infection rate, infectious period, lethality rate. Moreover, through such models, it is possible to estimate the number of

NOTE: This preprint reports new research that has not been certified by peer review and should not be used to guide clinical practice.

$R_0$ ) and during the epidemic evolution (effective time-dependent Reproduction number  $R_t$ ). In

21 particular, the trend of  $R_t$  is of great importance to check the epidemic evolution over time.

22 The COVID-19 pandemic, caused by the Sars-CoV-2 virus, has renewed interest in studying  
23 these models and a significant number of papers appeared on this subject since the beginning of  
24 2020 (refer to LitCovid database for up to date literature [1]). They differ each other for the  
25 type of model proposed, the external events considered, such as movement restrictions imposed by  
26 governments or quarantines, and the regions where models are applied.

27 Starting from the first SIR (Susceptible (S), Infected (I), and Recovered (R)) model, proposed  
28 in 1927 by Kermack and McKendrick [2], several generalizations have been formulated over the  
29 years by increasing the number of compartments, such as, for example, the Susceptible – Exposed –  
30 Infectious – Recovered (SEIR) and the Susceptible - Exposed - Infected - Recovered - Dead (SEIRD)  
31 schemes. Further extensions have been proposed to model the COVID-19 outbreak considering the  
32 different social distancing policies and control measures applied in the various geographic areas to  
33 contain the epidemic spread. More compartments have been added, making the models more and  
34 more complex (see [3], [4], [5], [6], to mention only a few of the most recent).

35 In this paper we intend to consider the effects of the vaccine on the epidemic spread by fur-  
36 ther extending the SEIRD model adding the compartment of Vaccinated people, thus obtaining  
37 a SEIRDV scheme. Among the vaccine-related papers within the COVID-19 literature several  
38 hypothetical scenarios are analysed based on different prioritisation policies according to vaccine  
39 efficacy and its availability [7]. Other papers focus on the possible benefits of combining vaccina-  
40 tion with Nonpharmaceutical Interventions (NPIs) such as surveillance, social distancing, social  
41 relaxation, quarantining, patient treatment/isolation (see [8, 9] and references therein).

42 Following the approach in [10], we introduce a switching rule that governs the SEIRDV model  
43 state at any given time. Besides producing optimal fit to epidemic data, introducing such a hy-  
44 brid approach allows us to represent disease evolution when restriction policies and virus variants  
45 cause changes in fundamental parameters such as infection rate, recovery periods, and death rates.  
46 Although switched models are widespread in various engineering applications, studies about epi-  
47 demic models are less common; see, for example, [11] (SIRV), [12](SIR) and [13] (SEIRD). In  
48 particular the authors in [13] propose a hybrid SEIRD model with a mortality rate represented  
49 by an inverse exponential function where the residual correction is based on the ARIMA method.  
50 The model, tested on US COVID statistic data in the period February-September 2020, made  
51 precise predictions for up to 2 months ahead. The reader can also refer to [13] for an exhaustive  
52 bibliography.

53 Concerning the model parameters, it is well known that COVID-19 epidemic data cannot  
54 be accurately represented by any compartmental approach with constant parameters all over the  
55 epidemic duration. To face this problem, some authors use variable parameters in the time interval  
56 (for example [6] ) or change the fitting function (see [5]). In our approach all the model parameters  
57 are constant in each switching time interval, except for the infection rate which is a time-dependent

58 forcing function modelled as piecewise continuous.

59 The model calibration is carried out by solving a sequence of constrained minimisations of the  
60 weighted least-squares residuals between the measured epidemic data and the value of the state  
61 variables, which satisfy the initial value ordinary differential system representing the SEIRDV  
62 model.

63 This paper is an extension of our previous work [14], where we proposed a SEIRD model (before  
64 the availability of vaccines), with two different forcing functions, to monitor the first phase of the  
65 evolution of Covid-19 in Italy (2020/02/24-2020/05/24). Compared to [14] we modify the model,  
66 by including the Vaccinated compartment (we remark that the vaccination campaign started in  
67 Italy on 27 December 2020), by representing the proposed model into the hybrid models' theoretical  
68 frame, and by changing the expression of the forcing functions. Moreover in the calibration phase,  
69 we add weights in the fitting objective function and bound constraints, thus improving the model  
70 computational effectiveness and accuracy.

71 In the experimental section, we report the results obtained by our scheme on the Italian national  
72 and regional epidemic data in the period 2020/12/27-2021/06/12. The inclusion of two different  
73 expressions for the infection rate function allows us to obtain different possible scenarios which  
74 prove to be very useful in the prediction phase.

### 75 *1.1. Contributions*

76 We summarize here the main contributions of this paper.

- 77 • We propose a SEIRDV scheme by adding the Vaccinated compartment to the well known  
78 SEIRD model.
- 79 • We consider a dynamical switched framework where the interval length is chosen on the basis  
80 of the Bayesian Information Criterium.
- 81 • We represent the infection rate as a continuous time dependent function comparing a linear  
82 and an exponential piecewise formulation.

83 The rest of the paper is organized as follows. In Section 2, we present the proposed model and  
84 the calibration procedure. The Section 3 reports the calibration results for the data of the COVID-  
85 19 in Italy and in the Emilia-Romagna region as well as possible forecast scenarios. Conclusions  
86 are drawn in Section 4.

## 87 **2. METHODS**

88 This section introduces the details of the proposed switched compartmental model and its al-  
89 gorithmic formulation. We start by describing the SEIRDV model in paragraph 2.1, then we intro-  
90 duce the switched model together with insights about the time-dependent infection rate functions

91 (paragraph 2.2). In paragraph 2.3, we discuss the algorithmic details of the calibration proce-  
92 dure consisting of a sequence of bound-constrained optimization problems defined by the model  
93 switches. Finally, in paragraph 2.4 we briefly discuss how we use the model to make predictions.

#### 94 2.1. The SEIRDV model with constant parameters

The SEIRDV model characterized by constant parameters is obtained from the SEIRD model [14] by adding the new compartment  $V$  representing the vaccinated population. The following differential system represents the populations' dynamics:

$$\begin{aligned}S' &= -\frac{\beta}{N}SI - \nu S, \\E' &= \frac{\beta}{N}SI - \alpha E \\I' &= \alpha E - \gamma I \\R' &= \gamma(1 - \eta)I \\D' &= \gamma\eta I \\V' &= \nu S\end{aligned}\tag{1}$$

95 where the total population, assumed of constant size  $N$ , is subdivided into six compartments: Sus-  
96 ceptible (S), Exposed (E), Infected (I), Recovered (R), Dead (D) and Vaccinated (V). The system  
97 (1) is solved starting from an initial time  $t = t_0$  where the values  $S(t_0), E(t_0), I(t_0), R(t_0), D(t_0), V(t_0)$   
98 are assigned on the basis of the available data and integrated up to a final time  $T$ .

99 The parameter  $\beta \geq 0$  represents the infection rate, accounting for the susceptible people in-  
100 fected by infectious people. Its value is related to the number of contacts between Susceptible and  
101 Infected. Standard models, as well as our SEIRDV, assume this relationship to be linear.

102 The parameter  $\alpha > 0$  represents the incubation rate for the transition from Exposed to Infected  
103 states. Such value relates to the incubation period  $A_I$  as follows:  $A_I = 1/\alpha$ . The average  
104 incubation ranges from 2 to 14 days ( $d$ ) (see <https://www.worldometers.info/coronavirus/coronavirus-incubation-period/>). According to [15], more than 97 percent of people who con-  
105 tract SARS-CoV-2 show symptoms within 11.5 days of exposure. Recently a comparative study  
106 assesses the incubation period around 6.5 days [16]. The cited studies assess the value of  $\alpha$  in the  
107 interval  $[0.14, 0.5]$ .

108  
109 The parameter  $\gamma > 0$  representing the removal rate relates to the average infectious period  $T_I$  as  
110  $\gamma = 1/T_I$ . At the beginning of the outbreak, an average value  $T_I \simeq 20d$  has been measured [17],  
111 hence  $\gamma \in [0.03, 0.1]$ .

112 After the period  $T_I$ , the Infected split into Recovered and Dead with weights  $1 - \eta$  and  $\eta$  respec-  
113 tively ( $0 \leq \eta \leq 1$ ). Hence the parameter  $\eta$  represents the fraction of the Removed individuals  
114 who die and its value depends on environmental situations that change over time, such as the

115 population age, the virus spread, medical care availability and treatments. Finally, the parameter  
116  $\nu > 0$  represents the vaccination rate. Its value is particularly useful in the prediction phase to  
117 obtain different scenarios.

118 Important information about the epidemic development is obtained from the number of infection  
119 cases generated from a single infectious individual, i.e. the basic reproduction number  $R_0$ , defined  
120 as follows (see details in appendix [Appendix B](#)):

$$R_0 = \frac{\beta}{\gamma}. \quad (2)$$

121 It is well known that the epidemic occurs when  $R_0 > 1$ ; however, this information refers to  
122 the initial stage, assuming that the entire population is Susceptible. In the case of COVID-19,  
123 estimations of  $R_0$  in the interval  $[1.5, 6.68]$  were obtained during the first months of 2020 [\[18\]](#).

## 124 2.2. Switched forced SEIRDV model

The movement restriction policies adopted worldwide as well as the occurrence of different virus variants cause changes in the value of the infection rate  $\beta$  and possibly of other model parameters over time. In order to monitor the model parameters from the measured data flexibly, we propose a *hybrid switched* version of the SEIRDV model and represent the infection rate  $\beta$  as a continuous time-dependent function, modelled according to the epidemic data. We split the time interval  $[t_0, T]$  into  $p$  sub-intervals  $\Delta_k = [t_{k-1}, t_k]$  ( $k = 1, \dots, p$  and  $t_p = T$ ) and define a switching rule  $\Theta$  setting the values of the model parameters as follows:

$$\Theta(t) = (\alpha_k, \beta_k, \gamma_k, \eta_k, \nu_k)^T, \quad t \in \Delta_k.$$

125 Then the hybrid model is represented as [\[10\]](#):

$$\begin{pmatrix} u' \\ \Theta' \end{pmatrix} = \begin{pmatrix} F_{\Theta}(t, u) \\ \mathbf{0} \end{pmatrix}, \quad u = (S(t), E(t), I(t), R(t), D(t), V(t)) \quad (3)$$

126 with state variable  $(u, \Theta)^T$  and  $F_{\Theta}(t, u)$  as in [\(1\)](#), and with model parameters represented by the  
127 piecewise constant function  $\Theta(t)$ .

128 However, using a constant value for the infection rate does not represent the epidemic behaviour  
129 in a sufficiently flexible way [\[14\]](#); therefore, we introduce a continuous time-dependent infection rate  
130  $\beta(t)$ . In this case, the epidemic model is known in the literature as *forced* model (see for example  
131 [\[19\]](#) chp 6). In this paper, we represent the infection rate as piecewise linear and exponential  
132 interpolating functions, yielding to SEIRDV\_pwl and SEIRDV\_pwe models, respectively.

133 Let us define  $\beta_k(t)$  the restriction of  $\beta(t)$  to the interval  $\Delta_k$ ,  $k = 1, \dots, p$ , and set the values

134  $\beta_k \equiv \beta(t_k)$ ,  $k = 0, \dots, p$ . The SEIRDV\_pwl defines the infection rate as:

$$\beta_k(t) = \frac{t - t_k}{t_{k-1} - t_k} \beta_{k-1} + \frac{t - t_{k-1}}{t_k - t_{k-1}} \beta_k, \quad t \in \Delta_k, \quad (4)$$

135 whereas SEIRDV\_pwe defines the infection rate as follows:

$$\beta_k(t) = \beta_{k-1} e^{-\rho(t-t_{k-1})/(t_k-t_{k-1})}, \quad \rho = -\log\left(\frac{\beta_k}{\beta_{k-1}}\right), \quad t \in \Delta_k. \quad (5)$$

We observe that for both models it holds :

$$\beta_k(t_k) = \beta_{k+1}(t_k), \quad k = 1, \dots, p-1$$

136 hence  $\beta$  is continuous in  $[t_0, T]$ .

137 The evolution of the global hybrid forced model, represented in figure 1, shows the changes  
 138 of the epidemic model at each switching interval  $\Delta_k$  represented by the values of the model parameters defined as  $\Theta_k \equiv \Theta(t), t \in \Delta_k$ . The restriction of the dynamical model (3) on each

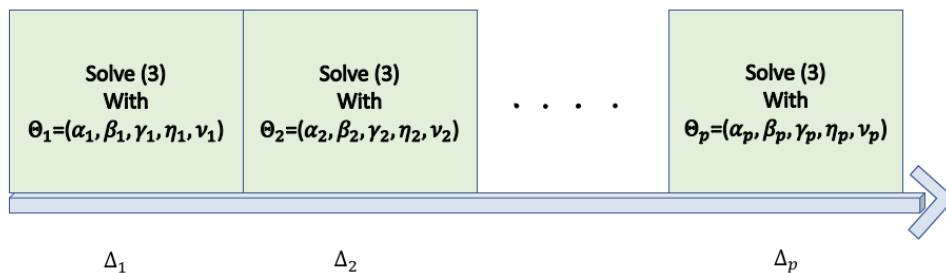


Figure 1: The evolution of the global hybrid model, related to the values of the parameters  $\Theta_k$ .

139

140 interval  $\Delta_k$ , is represented in Figure 2, where the model populations, for  $t \in \Delta_k$ , are given by  $(S_k, E_k, I_k, R_k, D_k, V_k)$ .

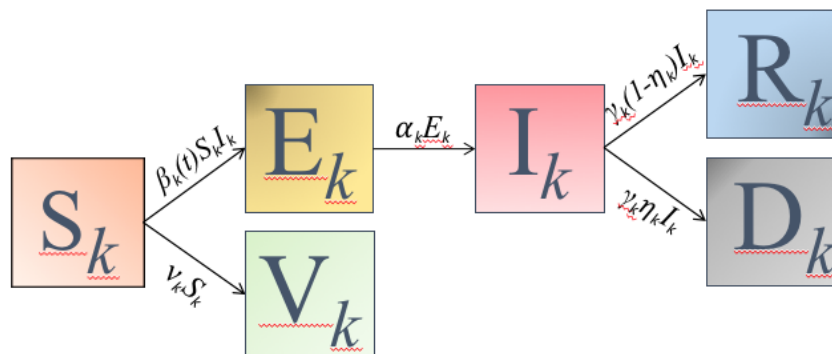


Figure 2: Dynamical model (3) restricted to the interval  $\Delta_k$ .

141

142 *2.3. Calibration Procedure*

143 This paragraph describes the calibration procedure in the interval  $[t_0, T]$  supposed of  $n$  days.  
 144 We calibrate the parameters on the sub-intervals  $\Delta_k$ ,  $k = 1, \dots, p$  with uniform size  $L = \lfloor n/p \rfloor$   
 145 (special care is taken in the case  $n \neq L \cdot p$  to avoid a too small length of  $\Delta_p$ ).

146 Generally, we are interested in keeping  $L$  as large as possible to guarantee a proper balancing  
 147 between the data fit and the model complexity, evaluated in terms of the number of parameters to  
 148 be calibrated. In section 3 we discuss the details of the choice of a proper value for  $L$ .

149 We describe now the parameter estimation process in a single sub-interval  $\Delta_k$ . We collect the  
 150 observed data about Infected, Recovered, Dead and Vaccinated compartments in vectors  $I, R, D$   
 151 and  $V$  of size  $L$  and stack them into the matrix  $Y \in \mathbb{R}^{L \times 4}$ ,  $Y = [I, R, D, V]$ . Then we consider  
 152  $Z \in \mathbb{R}^{L \times 4}$  as the restriction of  $u(t; \Theta)$  (defined in (3)) to the components  $I(t), R(t), D(t), V(t)$   
 153 computed in the measurement days in  $\Delta_k$  and we compute the model parameters  $\Theta_k$  solving a  
 154 weighted constrained nonlinear least squares problem of the form:

$$\Theta_k = \arg \min_{\Theta \in B} \sum_{j=1}^4 \sum_{i=1}^L (Z_{i,j} - Y_{i,j})^2 / \mu_j, \quad \mu_j = \frac{1}{L} \sum_{i=1}^L Y_{i,j}. \quad (6)$$

where the positive weights  $\mu_j$  are introduced to compensate different data scales. The bound set  $B$  is defined as

$$B = \{ \Theta \in \mathbb{R}^5 : lb_i \leq \theta_i \leq ub_i, i = 1, \dots, 5 \}$$

where the upper bounds  $ub_i = 1, i = 1 \dots, 5$  and lower bounds

$$lb = [10^{-4}, 10^{-4}, 10^{-4}, 0, 10^{-6}]$$

155 contain the values estimated in the literature.

156 To solve the minimization problem (6) numerically, we use iterative solvers as discussed in  
 157 section 3. Figure 3 schematically represents the calibration steps of the global hybrid model in the  
 158 whole interval  $[t_0, T]$ . The scheme highlights that the results  $\Theta_k$  of the minimization problem on  
 159  $\Delta_k$  is taken in input as starting guess in the minimization problem on  $\Delta_{k+1}$ .

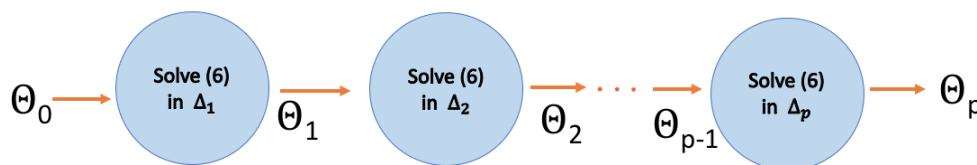


Figure 3: Calibration steps of the global hybrid model parameters  $\Theta_k$ .

160 To suitably choose the first starting guess  $\Theta_0$ , which has a fundamental role in the quality of  
 161 the final solution, we solve problem (6) on a unique short time interval  $T_i$  of about ten days with

162 starting guess  $(0.1, 0.1, 0.1, 0.1, 0.1)$ .

163 In Algorithm 1 we summarize the main steps of the calibration phase to estimate the parameters

164  $\Theta_k, k = 1 \dots, p$ .

---

**Algorithm 1** Calibration Algorithm

---

1. Compute the solution  $\tilde{\Theta}$  of problem (6) with starting guess  $(0.1, 0.1, 0.1, 0.1, 0.1)$  in the interval  $[t_0, t_0 + 10]$
  2. Set  $\Theta_0 = \tilde{\Theta}$ .
  3. for  $k = 1, \dots, p$  do
  4.     Compute  $\Theta_k$  as the solution of (6) in the sub-interval  $\Delta_k$  with starting guess  $\Theta_{k-1}$
  5. end
- 

165 The forward differential problem (1) is solved by a fourth order variable step Runge-Kutta  
166 method. The initial conditions in each sub-interval  $\Delta_k$  are given by the observed values of the  
167 compartments  $I, R, D, V$  in the initial day of  $\Delta_k$ . Concerning the starting value  $E_0$  of the Exposed  
168 compartment, which is not available from data, in the starting interval  $\Delta_1$ , we relate it with the  
169 delay time  $t_d$  between the contact with the infectious agent and the onset of symptoms or signs of  
170 infection, as follows:

$$E_0 = I(t_0 + t_d) - I(t_0). \quad (7)$$

171 (see Section 3 for more details on the values of  $t_d$ ). In the successive intervals  $\Delta_k, k > 1$ , we set  
172  $E_0$  as the last value of Exposed computed in the interval  $\Delta_{k-1}$ . The starting value of Susceptible  
173 is the difference between the total population  $N$  and the sum of all the other compartments.

#### 174 2.4. Prediction

175 We use SEIRDV to predict the future behaviour of the disease evolution in short-medium  $m$ -  
176 days interval  $[T, T_m]$ , with  $T_m = T + m$ . In this paper we have adopted the following two strategies  
177 for prediction.

- 178 1. We set in (1) the parameters  $\Theta_p = (\alpha_p, \beta_p, \gamma_p, \eta_p, \nu_p)$  computed in the last calibration interval  
179  $\Delta_p$  and we run the model over a unique time interval  $[T, T_m]$ . In our simulations we use both  
180 the SEIRDV\_pwl and SEIRDV\_pwe proposed approaches.
- 181 2. We set in (1) the parameters  $\Theta_\sigma = (\alpha_p, \beta_p, \gamma_p, \eta_p, \sigma \cdot \nu_p)$ , with  $\sigma > 1$ , to simulate an increased  
182 vaccination rate. We compute also in this case the prediction using both the linear and  
183 exponential  $\beta$  functions.

### 184 3. Numerical results

185 The results presented in this section have been obtained by implementing the SEIRDV\_pwl  
186 and SEIRDV\_pwe algorithms in Matlab 2021a. The codes are available on [https://github.com/](https://github.com/fzama63/COVID-SEIRDV)  
187 [fzama63/COVID-SEIRDV](https://github.com/fzama63/COVID-SEIRDV).



### 188 3.1. Data description

189 Epidemic data are downloaded from the repository open source Github [https://github.com/](https://github.com/pcm-dpc/COVID-19)  
190 [pcm-dpc/COVID-19](https://github.com/pcm-dpc/COVID-19) of the Italian Civil Protection Department, containing the official data provided  
191 by the Ministry of Health (see [20] for a detailed description). We consider here the global national  
192 data ( $N = 60360000$ ) as well as the regional data from Emilia-Romagna ( $N = 4445900$ ).

193 Information about vaccine administration is obtained in the Github repository: [https://](https://github.com/italia/covid19-opendata-vaccini)  
194 [github.com/italia/covid19-opendata-vaccini](https://github.com/italia/covid19-opendata-vaccini) (see details in Appendix A).

### 195 3.2. Model calibration

196 We have solved the constrained least squares problems (6) by means of the `lsqnonlin` Matlab  
197 function from the `Optimization Toolbox` with the trust-region reflective algorithm. The initial  
198 value differential problem (1) has been solved with the `ode45` Matlab function.

To analyse the numerical solution of the calibration in the interval  $[t_0, T]$  constituted of  $n$  days,  
we compute, for any considered population, a Relative RESidual defined as:

$$RRES = \frac{\sum_{i=1}^n (X_i - Xd_i)^2}{\sum_{i=1}^n Xd_i^2}$$

and the Bayesian Information Criterion (BIC) [21], defined as follows:

$$BIC = N_\theta \log(n) + \log\left(\frac{\sum_{i=1}^n (X_i - Xd_i)^2}{n}\right)$$

199 where  $N_\theta$  is the number of the estimated parameters,  $Xd_i$  represents the acquired compartment  
200 data and  $X_i$  is the corresponding value computed by the calibrated model at day  $i$ ,  $i = 1, \dots, n$ .  
201 The *BIC* takes into account the number of model estimated parameters and tends to penalize the  
202 inclusion of additional parameters. The lower this quantity, the better the model will be.

203 To set a convenient initial value  $E_0$  for the Exposed compartment we run `SEIRDV_pwl` and  
204 `SEIRDV_pwe` on the first 15 days, from 2020/12/27 to 2021/01/10, choosing  $E_0$  as in (7) with  $t_d =$   
205  $1, \dots, 10$  days. Then we compute *RRES* for the Infected compartment and choose  $t_d$  corresponding  
206 to the minimum value. As shown in figure 4, the smallest *RRES* is obtained when  $t_d = 2$  for both  
207 `SEIRDV_pwl` and `SEIRDV_pwe`, hence we continue with  $t_d = 2$  throughout this section.

208 We define the calibration period of  $n = 85$  days, from 2020/12/27 to 2021/3/21 (we remind  
209 that in Italy vaccination campaign started on 2020/12/27) and run the calibration of `SEIRDV_pwe`  
210 and `SEIRDV_pwl` models.

211 The first aspect of our analysis concerns the choice of the number of switches. We split the whole  
212 time interval into sub-intervals of fixed length  $L$  (except for the last one which can be of different  
213 size). By increasing their number, we decrease the fit error at the expense of the computation cost,  
214 determined by the number of parameters, proportional to the number of switches. In order to  
215 choose the best value  $L$  we try all the values in the interval  $[5, 85]$  days, we compute the minimum

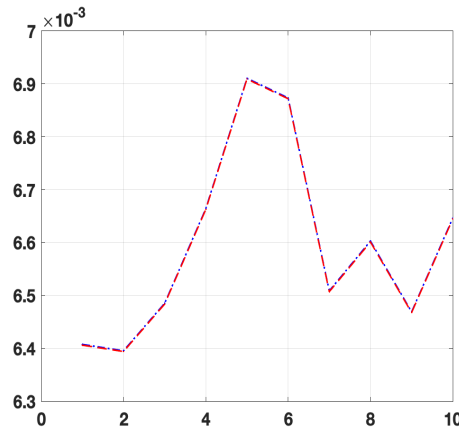


Figure 4:  $RRES$  vs  $t_d$  for SEIRDV\_pwl (blue dash-dotted line) and SEIRDV\_pwe (red dashed line)

216  $BIC_{min}$  over all BIC values and we evaluate:  $\Delta_{BIC} = BIC_X - BIC_{min}$  where X is any of the  
 217 considered populations (I,R,D or V).

218 In Figure 5 we plot the value  $\Delta_{BIC}$  vs  $L$  for each compartment: red dot-dashed line for  
 219 SEIRDV\_pwe and blue line for SEIRDV\_pwl model. Except for the Vaccinated (figure 5(d)), all  
 220 the populations show the minimum  $BIC$  for  $L = 21$ .

Hence throughout this section, we split the calibration time into four sub-intervals of length  
 $L = 21$  obtaining the following time intervals:

$$\begin{aligned} \Delta_1 &= [2020/12/27, 2021/01/21] & \Delta_2 &= [2021/01/17, 2021/02/07] \\ \Delta_3 &= [2021/02/07, 2021/02/28] & \Delta_4 &= [2021/02/28, 2021/03/21]. \end{aligned} \quad (8)$$

221 We calibrate the model parameter using Algorithm 1. For the solution of the constrained  
 222 optimization problem, we compared the `trust-region reflective` (TR) method with the Lev-  
 223 emberg Marquardt (LM) one, which overperforms the Broyden-Fletcher-Goldfarb-Shanno (BFGS)  
 224 as noted in [5]. We report in Table 1 the number of function evaluations FCount and the relative  
 225 residual  $RRES$  for the Infected, Recovered, Dead and Vaccinated compartments. We find that for  
 226 both exponential and linear infection rates, the TR method is computationally the most efficient  
 227 (smallest number of function evaluations) and it is also slightly more precise than LM. Therefore  
 we continue our analysis applying the TR method.

model	method	FCount	$RRES$			
			I	R	D	V
SEIRDV_pwl	TR	<b>126</b>	<b>0.0084</b>	<b>0.0019</b>	<b>0.0010</b>	0.0381
	LM	3926	0.0087	0.0021	0.0015	0.0381
SEIRDV_pwe	TR	<b>132</b>	<b>0.0083</b>	<b>0.0019</b>	<b>0.0010</b>	0.0381
	LM	4192	0.0085	0.0020	0.0014	0.0381

Table 1: Number of function evaluations FCount and relative residual  $RRES$  obtained by LM and TR solvers for SEIRDV\_pwl and SEIRDV\_pwe. In bold the best results obtained for each algorithm.

228

229 Figures 6 (a) and 7 (a) and (b) plot the calibrated functions of Infected, Recovered and Vac-

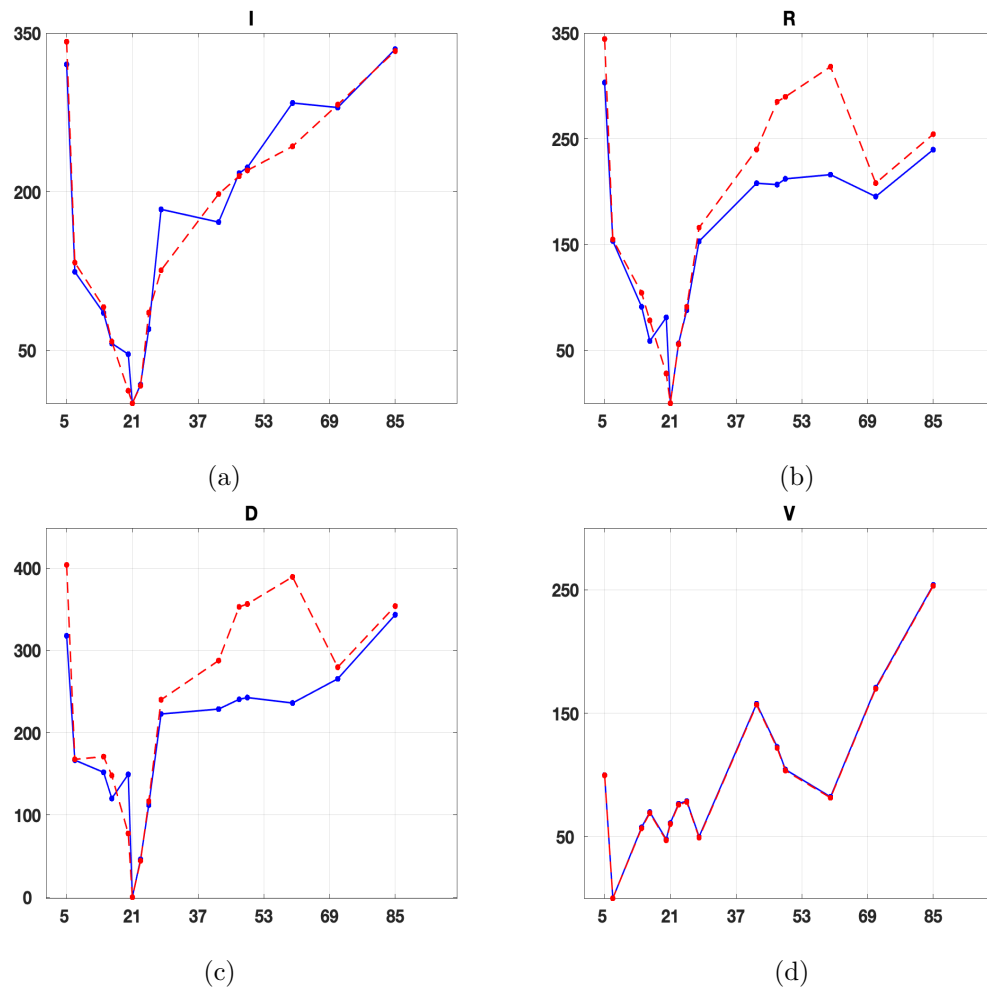


Figure 5:  $\Delta_{BIC}$  vs  $L$  for each compartment: red dot-dashed line for SEIRDV\_pwe and blue line for SEIRDV\_pwl model. (a) Infects (b) Recovered (c) Dead (d) Vaccinated.

230 cinated populations, respectively. We can appreciate the good quality of data-fit of SEIRDV\_pwl  
 231 and SEIRDV\_pwe. In Figure 6 (b) we represent the difference between the infected population ob-  
 232 tained by SEIRDV\_exp and SEIRDV\_pwl algorithms. We observe that the main differences occur  
 in the  $\Delta_3$  and  $\Delta_4$  intervals.

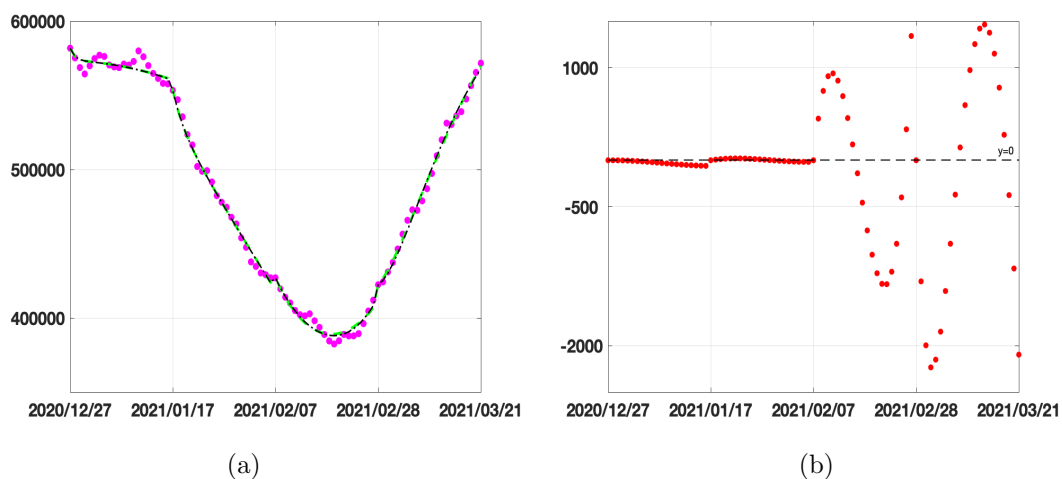


Figure 6: Calibration results on Infected compartment. (a) Data from 2020/12/27 until 2021/03/21 (magenta circles), SEIRDV\_pwl calibration (black dashed line), SEIRDV\_pwe calibration (green continuous line). (b) Difference between SEIRDV\_pwe and SEIRDV\_pwl (red circles).

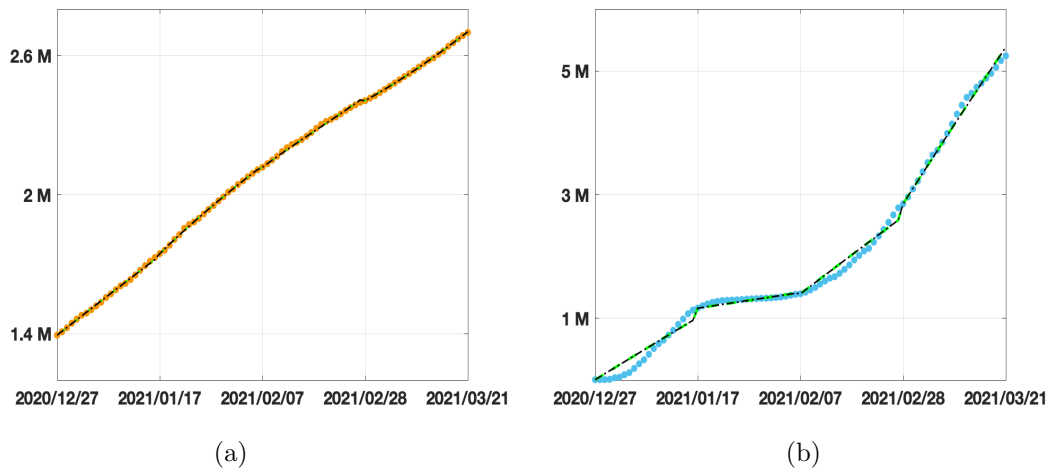


Figure 7: Calibration results. (a) Recovered compartment. Data from 2020/12/27 until 2021/03/21 (orange circles), SEIRDV\_pwl calibration (black dashed line), SEIRDV\_pwe calibration (green continuous line). (b) Vaccinated compartment. Data from 2020/12/27 until 2021/03/21 (cyan circles), SEIRDV\_pwl calibration (black dashed line), SEIRDV\_pwe calibration (green continuous line).

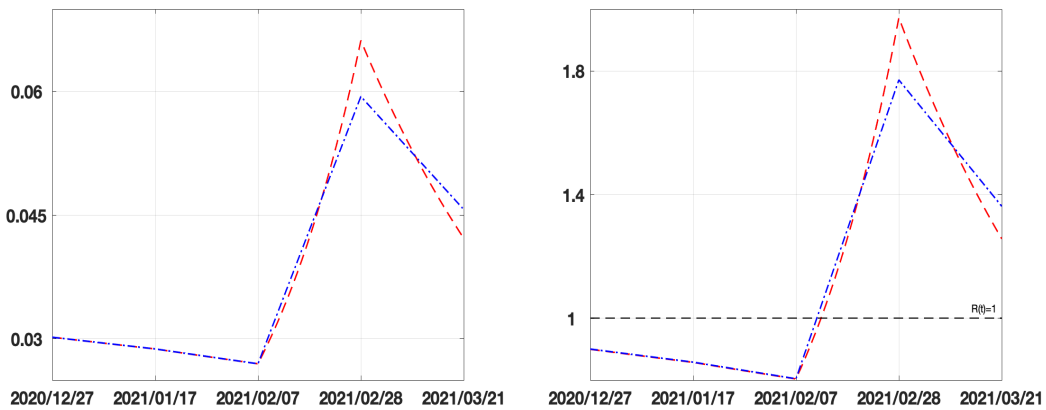


Figure 8: Forcing  $\beta$  functions (on the left) and Reproduction index  $R_t$  (on the right) for SEIRDV\_pwl (blue dash-dotted line) and SEIRDV\_exp (red dashed line) models.

233 In Figure 8 we plot the values of both the infection rate function  $\beta(t)$  (on the left) and the  
 234 reproduction number function  $R_t(t)$  (on the right) computed as follows

$$R_t = \frac{\beta(t)}{\hat{\gamma}}, \quad \hat{\gamma} = \frac{1}{p} \sum_{k=1}^p \gamma_k. \quad (9)$$

235 The red line relative to the exponential model changes more rapidly when the epidemic spread  
 236 increases ( $\Delta_3$  and  $\Delta_4$  intervals). To analyse the behaviour of the infection rate in the considered  
 237 sub-intervals, we average the values of the calibrated function  $\beta(t)$ , represented in figure 8 (a), on  
 238 the intervals  $[\Delta_1, \Delta_2]$ , getting 0.00286 for both the methods, and in the period  $[\Delta_3, \Delta_4]$  obtaining  
 239 0.0480 and 0.0487 for SEIRDV\_pwl SEIRDV\_pwe, respectively. These values show that both  
 240 methods capture the increase of the infection rate that causes the inversion of the epidemic curve  
 241 in  $[\Delta_3, \Delta_4]$ .

242 We now discuss the parameters calibrated by Algorithm 1 and reported in Table 2. Concerning  
 243 the incubation rate  $\alpha$ , both models report a decreasing behaviour in the period  $\Delta_1 - \Delta_4$ . It  
 244 corresponds to an incubation period between 2 and 4 days. The removal rate  $\gamma$  is very similar  
 245 for both methods and gives the following removal periods: 34  $d(\Delta_1)$ , 25.9  $d(\Delta_2)$ , 26.9  $d(\Delta_3)$ ,  
 246 34.2  $d(\Delta_4)$  producing the average removal period of 30.3  $d$ .  
 247 Regarding the parameter  $\eta$ , we observe that the average value 2.4% obtained by SEIRDV\_pwl  
 248 slightly underestimates the reference value 3%, reported by Johns Hopkins University Coronavirus  
 249 Resource Center, <https://coronavirus.jhu.edu/data/mortality>. On the contrary, the average  
 250 value 3.2% obtained by SEIRDV\_pwe constitutes a slight overestimate. Both models compute the  
 251 same vaccination rate  $\nu$  in each period.

parameter	model	$\Delta_1$	$\Delta_2$	$\Delta_3$	$\Delta_4$	mean
$\alpha$	SEIRDV_pwl	0.9790	0.4293	0.3217	0.2571	0.4968
	SEIRDV_pwe	0.9790	0.4297	0.3433	0.2276	0.4949
$\gamma$	SEIRDV_pwl	0.0294	0.0386	0.0371	0.0293	0.0336
	SEIRDV_pwe	0.0294	0.0386	0.0372	0.0293	0.0336
$\eta$	SEIRDV_pwl	0.0290	0.0238	0.0216	0.0238	0.0245
	SEIRDV_pwe	0.0294	0.0386	0.0372	0.0293	0.0336
$\nu$	SEIRDV_pwl	0.0008	0.0002	0.0010	0.0022	0.0011
	SEIRDV_pwe	0.0008	0.0002	0.0010	0.0022	0.0011

Table 2: Parameters calibrated in the different time intervals (8).

### 252 3.3. Prediction on national data

253 In this paragraph, we apply the calibrated SEIRDV\_pwl and SEIRDV\_pwe to make predictions.  
 254 To test the forecast reliability, we compute a prediction in the interval  $\Delta_5 = [2021/03/21, 2021/04/20]$   
 255 using the data available in that period to measure the precision of our forecast in terms of the  
 256 Infected peak time and value.

257 In Figure 9 we show the predicted Infected curve. With the red dashed curve we plot the  
 258 prediction obtained by using the values of all the parameters calibrated in the last interval  $\Delta_4$ .  
 259 With the continuous blue line, we plot the prediction obtained by changing only the  $\beta(t)$  function as  
 260 the curve interpolating the infection rate calibrated in 2021/02/28 and 2021/03/21 (drawn with a  
 261 blue and a red star, respectively). Comparing the prediction curves relative to SEIRD\_pwl (Figure  
 262 9 (a)) and SEIRD\_pwe (Figure 9 (b)) with the epidemic data represented by magenta empty circles  
 263 we can see that the exponential model is more accurate.

264 We highlight that the reported forecast refers to the vaccination rate  $\nu = 0.0022$ , computed in  
 265 the calibration interval  $\Delta_4$  corresponding to 133572 administration per day. From Table 3 we can  
 266 see that the peak of infected people is reached on 2021/04/09 and 2021/04/03 with SEIRD\_pwl and  
 267 SEIRD\_pwe predictions, respectively. We observe that SEIRD\_pwe curve is closer to the available  
 268 data that reaches its maximum on (2021/03/28) with 573235 Infected people.

269 In the second and third lines of the table, we report the maximum number of Infected and  
 270 the day of forecast peak increasing the vaccination rate. To graphically represent the effects of an

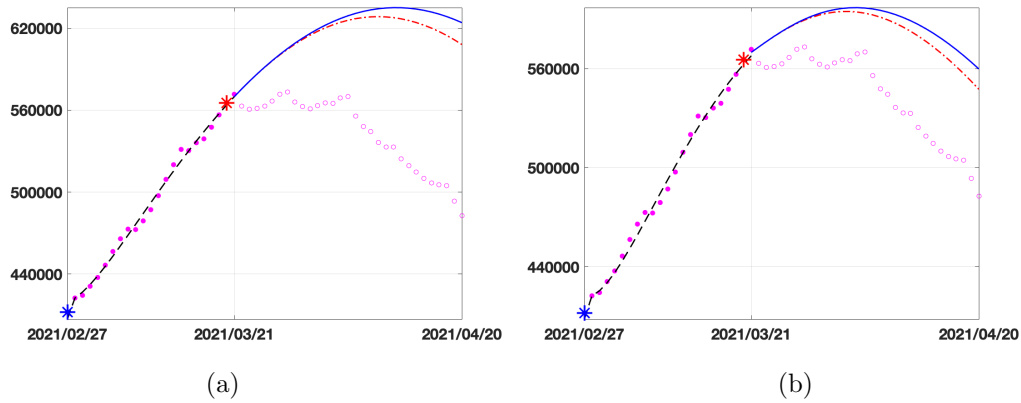


Figure 9: Prediction for the Infected compartment in Italy from 2021/03/22 to 2021/04/20. Data (magenta circles), prediction with  $\beta(t)$  calibrated in the last interval  $\Delta_4$  (red dashed line) and prediction with  $\beta(t)$  interpolating the values of  $\beta$  in red and blue stars (blue continuous line). (a) SEIRDV\_pwl (b) SEIRDV\_pwe

vaccination rate	administration per day	SEIRDV_pwl		SEIRDV_pwe	
		#(Infected)	peak day	#(Infected)	peak day
0.0022	133572	628504	09/04/21	594604	03/04/21
0.0055	333930	622139	07/04/21	592549	01/04/21
0.0088	534288	617322	05/04/21	590882	01/04/21

Table 3: Results of the prediction experiment in Italy obtained with different vaccination rates: number of Infected people and day of the peak for SEIRDV\_pwl and SEIRDV\_pwe. The peak of available data is on 2021/03/28 with 573235 Infected people.

271 increased vaccination rate, we plot in Figure 10 the results given by the two models in 40 days  
 272 using the vaccination rates in Table 3. Comparing the two models, we see that the SEIRDV\_pwe  
 273 gives the more realistic prediction.

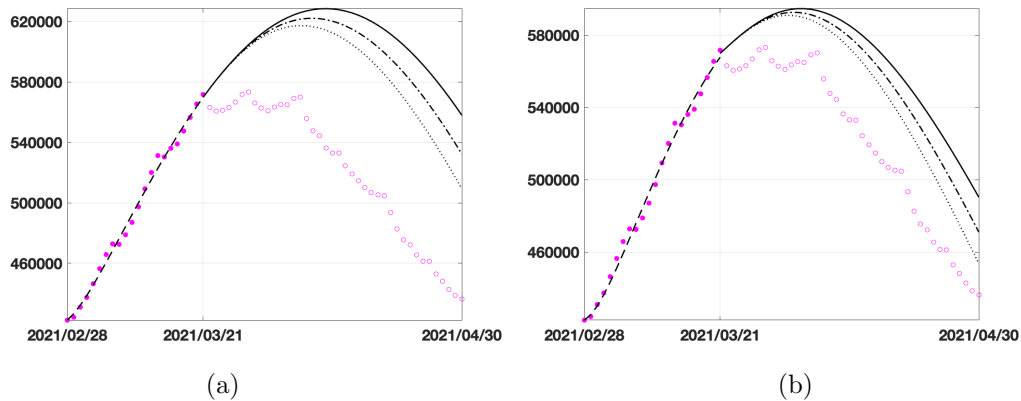


Figure 10: 30 days prediction for the Infected compartment in Italy by considering different vaccination rates  $v = 0.0022129$  (dark continuous line),  $v = 0.0055323$  (dark dashed-dotted line) and  $v = 0.0088517$  (dark dotted line) : (a) SEIRDV\_pwl, (b) SEIRDV\_pwe

### 274 3.4. Prediction on regional data

275 Finally, we present the prediction obtained using more homogeneous and smaller-scale data  
 276 acquired in the Emilia-Romagna region after performing the calibration on the same sub-intervals  
 277 as in (8). In Figure 11 we plot the prediction obtained with the same procedure as in Figure 9.  
 278 Differently to what happens for the Italian case, in the linear model (Figure 11 (a)) the prediction

279 obtained with the red curve is entirely inaccurate, whereas for the exponential model (Figure 11  
 280 (b)) the red and blue lines define a region containing the Infected data. Therefore, SEIRDV\_pwe  
 281 can be used to make reliable predictions with both strategies. Finally, in Figure 12 we show the  
 282 results for increasing vaccination rates, as done in Figure 10 for the national data. The SEIRDV\_pwl  
 283 forecasts are now closer to the Infected data compared to SEIRDV\_pwe, confirming the importance  
 of having both methods available to make different predictions.

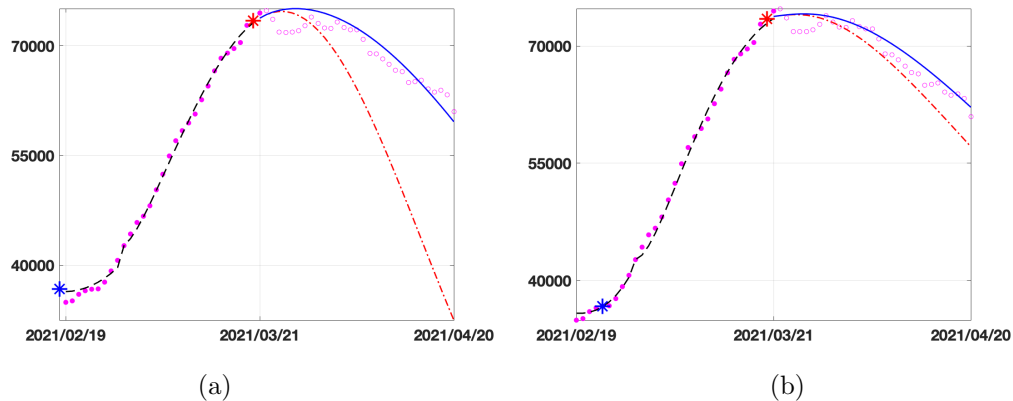


Figure 11: Prediction for the Infected compartment in Emilia-Romagna from 2021/03/22 to 2021/04/20. Data (magenta circles), prediction with  $\beta(t)$  interpolating the the values of  $\beta$  in red and blue stars (blue continuous line), prediction with  $\beta(t)$  calibrated in the last interval  $\Delta_4$ . (a) SEIRDV\_pwl (b) SEIRDV\_pwe

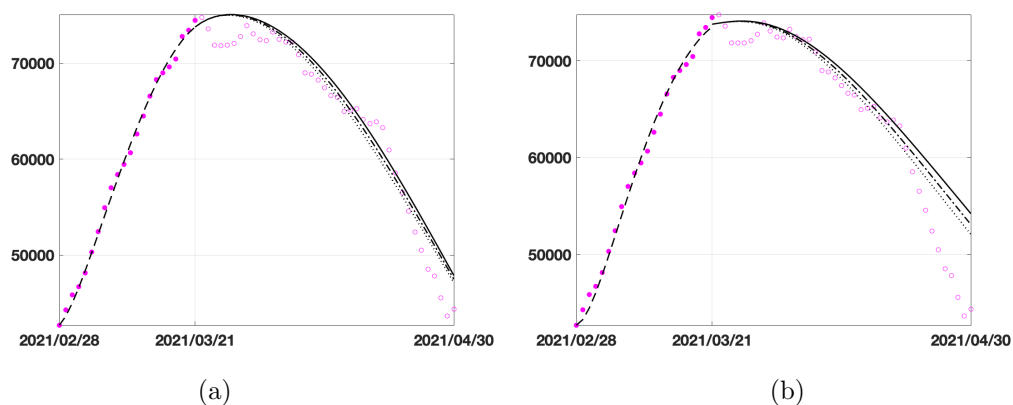


Figure 12: 30 days prediction for the Infected compartment in Emilia-Romagna by considering different vaccination rates  $v = 0.0022129$  (dark continuous line),  $v = 0.0055323$  (dark dashed-dotted line) and  $v = 0.0088517$  (dark dotted line) : (a) SEIRDV\_pwl, (b) SEIRDV\_pwe

284

### 285 3.5. Towards the 80% vaccination

286 In this experiment we extend the calibration period to the present date (2021/06/12) (using  
 287  $L = 21$  as in the previous experiments and  $p = 8$ ) and run the simulations to forecast the time at  
 288 which 70% – 80% population has received at least the first vaccine dose. As already observed, the  
 289 two models have a very similar behaviour concerning the fit of vaccinated population and the last  
 290 estimated vaccination rate is  $\nu = 0.0095$  for both SEIRDV\_pwl and SEIRDV\_pwe, equivalent to  
 291 584861 administrations per day. Hence we report in figure 13(a) the vaccination data (pink circles),  
 292 the fitted vaccinated population (black dashed line), together with the forecasts obtained with the

293 calibrated vaccination rate (black continuous line) and with an increased vaccination rate 30% (dot  
 294 dashed line) and 60% (dotted line) (computed by SEIRDV\_pwe). We highlight with dashed lines  
 295 the values of vaccinated individuals corresponding to 70% and 80% of the whole population. The  
 296 reproduction number  $R_t$  shown in Figure 13(b), obtained by calibrated data, confirms the positive  
 297 effects of the current vaccination campaign. The progressive decrease of  $R_t$  below 1 yields the  
 reduction of the disease spread. The expected similarity between SEIRDV\_pwl and SEIRDV\_pwe

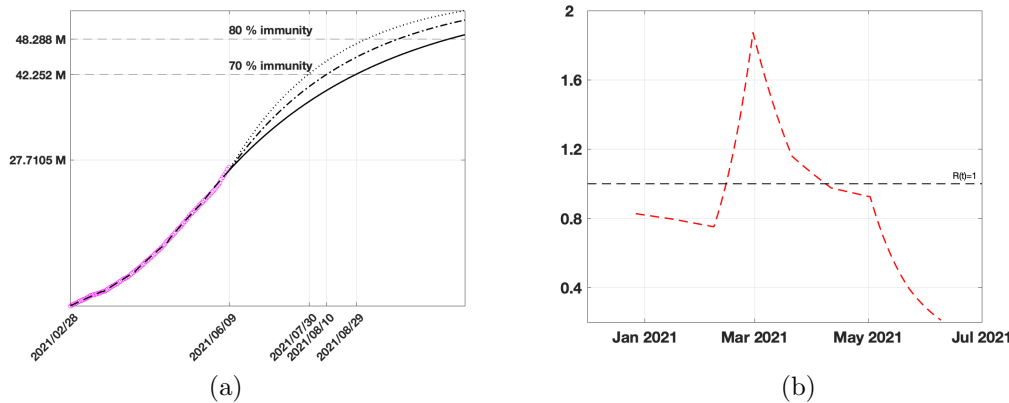


Figure 13: (a) Vaccination data (pink circles), fitted Vaccinated (black dashed line), forecast obtained by SEIRDV\_pwe considering the calibrated vaccination rate (black continuous line), an increase of 30% (dot dashed line) and 60% (dotted line) of vaccination rate. (b) Reproduction number  $R_t$ .

298

299 forecasts is confirmed by data reported in table 4, where the unique small difference appears in the  
 300 first row. The increase of 60% in the vaccination rate causes a reduction of one month to obtain  
 301 70% vaccinated population and about two months (57 d) for 80%.

vaccination rates	administration per day	SEIRDV_pwl		SEIRDV_pwe	
		70%	80%	70%	80%
0.0095	584861	29/08/21	28/10/21	29/08/21	27/10/21
0.0123	760319	10/08/21	25/09/21	10/08/21	25/09/21
0.0152	935778	30/07/21	05/09/21	30/07/2	05/09/21

Table 4: Results of the prediction experiment in Italy obtained by the vaccination rate (first row) calibrated on 12/06/2021 and with a 30% and 60% increase. Dates at which a single vaccine dose is given to 70% – 80% people.

Target	$\nu$	SEIRDV_pwl		SEIRDV_pwe	
		I	D	I	D
70%	0.0095	39716	129425	8890	128655
	0.0123	47873	129038	18386	128552
	0.0152	55545	128785	27912	128448
80%	0.0095	15895	130048	906	128739
	0.0123	19791	129621	3111	128712
	0.0152	24829	129346	6713	128672

Table 5: Value of Infected and Dead individuals correspondent to 70% and 80% immunization targets for the vaccination rates  $\nu$  displayed in table 4

302 The differences between the two models can be observed in table 5 reporting the number of  
 303 Infected and Dead individuals in the days of the vaccination targets 70%, 80% reported in table  
 304 4. Increasing the vaccination rate  $\nu$ , we observe a reduction of the Dead individuals for each



305 target and both methods. For each target and vaccination rate, the Infected and Dead individuals  
 306 computed by SEIRDV\_pwe are smaller than SEIRDV\_pwl.

307 The pie graph of Figure 14 shows the percentage of people of all the compartments corre-  
 308 sponding to 70% and 80% vaccination targets. In particular Figure 14 (a) represents SEIRDV\_pwl  
 309 reaching 70% vaccination target on 2021/08/29, at the calibrated vaccination rate ( $\nu = 0.0095$ )  
 310 whereas Figure 14 (b) is relative to SEIRDV\_pwe reaching 80% vaccination target on 2021/09/05  
 311 at the 60% increased vaccination rate ( $\nu = 0.0152$ ). The 10% increase in the Vaccination target  
 312 causes the same percentage reduction of the susceptible individuals from 23% to 13%, whereas  
 313 the percentages in the remaining populations do not change significantly. We can consider these  
 314 pictures as worse and best case predictions of the vaccination campaign in Italy.

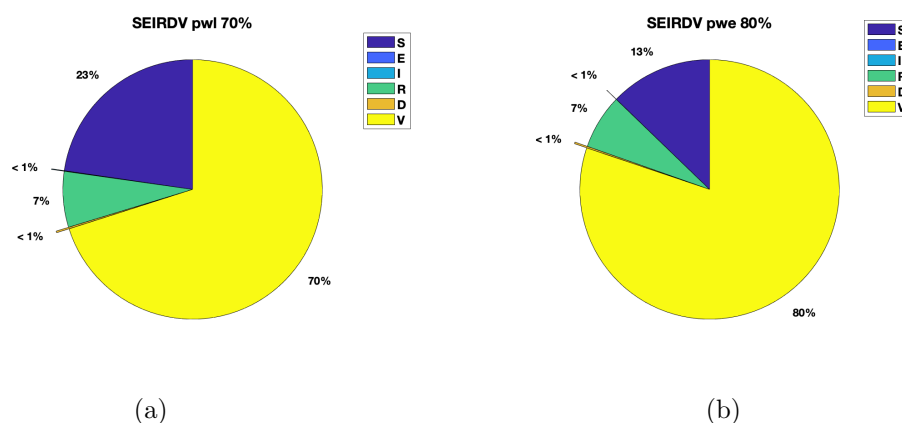


Figure 14: Percentage compartments obtained by SEIRD\_pwl on 2021/08/29 (a) and SEIRD\_pwe on 2021/09/05 (b).

#### 315 4. Conclusions

316 We have proposed two SEIRDV compartmental models, each involving six populations (Suscep-  
 317 tibles, Exposed, Infected, Recovered, Dead and Vaccinated) for the analysis of COVID-19 spread  
 318 during the vaccination campaign in Italy. The two schemes differ in the forcing time-dependent  
 319 function.

320 We have calibrated the model parameters in time intervals of about 20 days through a nonlinear  
 321 constrained least squares minimization. The results on the data on whole Italy and especially on  
 322 the Emilia-Romagna region are very promising. The data fit obtained is really very faithful with  
 323 both models for all the considered compartments with a relative residual value less than 1%. The  
 324 forcing functions, linear and exponential, characterize the model especially when the epidemic  
 325 spread is increasing.

326 The simulated predictions of the infected population behaviour in a 30 days period from mid  
 327 March to mid April 2021 show that the SEIRDV\_exp model performs better when compared with  
 328 the data available in that period. In particular, in the case of Emilia-Romagna we remark that the  
 329 peak day for the infected population is predicted with great accuracy. Simulations of the Infected

330 curve with a different, increasing, vaccination rate in the same period give the idea of how the  
331 epidemic would evolve in these cases.

332 Finally, we applied the model calibrated up to 2021/06/12 to forecast the epidemic behaviour  
333 when 70% – 80% of population has received one vaccine dose. At the present vaccination rate the  
334 80% immunization is reached on 2021/10/28 whereas with an increase of 60% (best scenario) it is  
335 reached on 2021/09/05.

336 Future studies and extensions of the proposed models will consider the limited duration of  
337 vaccine-induced immunity and the possible seasonal pattern of the COVID-19 epidemic waves.

## 338 **Appendix A. Vaccines Database Description**

339 We consider the file 'somministrazioni-vaccini-summary-latest.csv' in the folder 'dati'. It con-  
340 tains a table made of 16 fields:

341

<b>FIELD NAME</b>	<b>DATA TYPE</b>
<b>index</b>	Integer
<b>area</b>	String
<b>data_somministrazione</b>	Datetime
<b>totale</b>	Integer
<b> Sesso_maschile</b>	Integer
<b> Sesso_femminile</b>	Integer
<b>categoria_operatori_sanitari_sociosanitari</b>	Integer
<b>categoria_personale_non_sanitario</b>	Integer
<b>categoria_ospiti_rsa</b>	Integer
<b>categoria_over80</b>	Integer
<b>prima_dose</b>	Integer
<b>seconda_dose</b>	Integer
<b>codice_NUTS1</b>	String
<b>codice_NUTS2</b>	String
<b>codice_regione_ISTAT</b>	Integer
<b>nome_regione</b>	String

343

344

345 Although some vaccines are administered in two different doses we consider, in our model, as  
346 vaccinated the people who received at least the first dose. Since some studies report that the  
347 positive immunity effects obtained from a single dose are evident in the immediate days after the  
348 vaccine, we can use this information for our short-term prevision.

## 349 Appendix B. Reproduction Number $R_0$

Concerning the analysis of stability, equilibrium solutions of an SEIR model with different vaccination policies please refer to [22] and references therein. Using the relation  $N = S(t) + E(t) + I(t) + R(t) + D(t) + V(t)$ , we can eliminate the last equation in (1) and define a disease free equilibrium  $(S^*, E^*, I^*, R^*, D^*)$ , with  $I^* = E^* = R^* = D^* = 0$ . Following the next generation matrix approach [23, 24], we compute the basic Reproduction Number  $R_0$ , defined as the number of secondary cases generated by a single Infected. Let  $X = [E, I]^T$  be the state at infection of system (1), then the Exposed and Infected equations can be written as:  $X' = F(X) + W(X)$  where

$$F(X) = \begin{pmatrix} \beta SI/N \\ 0 \end{pmatrix}, \quad W(X) = \begin{pmatrix} \alpha E \\ -\alpha E + \gamma I \end{pmatrix}$$

The Jacobian matrices of  $F$  and  $W$  at the disease free equilibrium are:

$$\mathbf{F} = \begin{pmatrix} 0 & \beta S^*/N \\ 0 & 0 \end{pmatrix}, \quad \mathbf{W} = \begin{pmatrix} \alpha & 0 \\ -\alpha & \gamma \end{pmatrix}$$

According to [23] the basic reproduction number  $R_0$  is the maximum eigenvalue of the next generation matrix  $NGM = \mathbf{F}\mathbf{W}^{-1}$ , i.e.

$$NGM = \mathbf{F} \begin{pmatrix} 1/\alpha & 0 \\ 1/\gamma & 1/\gamma \end{pmatrix} = \frac{S^*\beta}{N\gamma} \begin{pmatrix} 1 & 1 \\ 0 & 0 \end{pmatrix}$$

350 In the assumption that at disease free state  $S^* = N$  we obtain (2). We note that it coincides with  
351 the  $R_0$  value of a standard SEIR model [19].

## 352 References

- 353 [1] Qingyu Chen, Alexis Allot, and Zhiyong Lu. LitCovid: an open database of COVID-19  
354 literature. *Nucleic Acids Research*, 49(D1):D1534–D1540, 11 2020.
- 355 [2] Kermack W.O. and McKendrick A.G. A contribution to the mathematical theory of epidemics.  
356 In *Proceedings of the Royal Society of London*, volume A, pages 700–721, 1927.
- 357 [3] Nicola Parolini, Luca Dede', Paola Antonietti, Giovanni Ardenghi, Andrea Manzoni, Edie  
358 Miglio, Andrea Pugliese, Marco Verani, and Alfio Quarteroni. Suihter: A new mathematical  
359 model for covid-19. application to the analysis of the second epidemic outbreak in italy, 2021.
- 360 [4] Jie Zhu and Blanca Gallego. Evolution of disease transmission during the covid-19 pandemic:  
361 patterns and determinants. *Scientific Reports*, 11(1):1–9, 2021.

- 362 [5] Hamdi Friji, Raby Hamadi, Hakim Ghazzai, Hichem Besbes, and Yehia Massoud. A gener-  
363 alized mechanistic model for assessing and forecasting the spread of the covid-19 pandemic.  
364 *IEEE Access*, 9:13266–13285, 2021.
- 365 [6] Giulia Giordano, Marta Colaneri, Alessandro Di Filippo, Franco Blanchini, Paolo Bolzern,  
366 Giuseppe De Nicolao, Paolo Sacchi, Patrizio Colaneri, and Raffaele Bruno. Modeling vacci-  
367 nation rollouts, sars-cov-2 variants and the requirement for non-pharmaceutical interventions  
368 in italy. *Nature Medicine*, pages 1–6, 2021.
- 369 [7] Satyaki Roy, Ronojoy Dutta, and Preetam Ghosh. Optimal time-varying vaccine allocation  
370 amid pandemics with uncertain immunity ratios. *IEEE Access*, 9:15110–15121, 2021.
- 371 [8] Manuel Adrian Acuña-Zegarra, Saúl Díaz-Infante, David Baca-Carrasco, and Daniel Olmos  
372 Liceaga. Covid-19 optimal vaccination policies: a modeling study on efficacy, natural and  
373 vaccine-induced immunity responses. *Mathematical Biosciences*, page 108614, 2021.
- 374 [9] Nikolaos P Rachaniotis, Thomas K Dasaklis, Filippos Fotopoulos, and Platon Tinios. A two-  
375 phase stochastic dynamic model for covid-19 mid-term policy recommendations in greece: a  
376 pathway towards mass vaccination. *International journal of environmental research and public  
377 health*, 18(5):2497, 2021.
- 378 [10] Rafal Goebel, Ricardo G Sanfelice, and Andrew R Teel. *Hybrid dynamical systems*. Princeton  
379 University Press, 2012.
- 380 [11] Liu X. and Stechliniski P. Infectious disease models with time-varying parameters and general  
381 nonlinear incidence rate. *Applied Mathematical Modelling*, 36(5):1974–1994, 2012.
- 382 [12] Amine El Koufi, Abdelkrim Bennar, and Noura Yousfi. Dynamics behaviors of a hybrid  
383 switching epidemic model with levy noise. *Appl. Math*, 15(2):131–142, 2021.
- 384 [13] Maher Ala’raj, Munir Majdalawieh, and Nishara Nizamuddin. Modeling and forecasting of  
385 covid-19 using a hybrid dynamic model based on seird with arima corrections. *Infectious  
386 Disease Modelling*, 6:98–111, 2021.
- 387 [14] Elena Loli Piccolomini and Fabiana Zama. Monitoring italian covid-19 spread by a forced  
388 seird model. *PLOS ONE*, 15(8):1–17, 08 2020.
- 389 [15] Lauer S.A., Grantz K.H., Bi Q., Jones F.K., Zheng Q., Meredith H.R., Azman A.S., Reich  
390 N.G., and Lessler J. The incubation period of coronavirus disease 2019 (covid-19) from publicly  
391 reported confirmed cases: Estimation and application. *Ann Intern Med.*, 172(9):577–582, 2020.
- 392 [16] Muluneh Alene, Leltework Yismaw, Moges Agazhe Assemie, Daniel Bekele Ketema, Wodaje  
393 Gietaneh, and Tilahun Yemanu Birhan. Serial interval and incubation period of covid-19: a  
394 systematic review and meta-analysis. *BMC Infectious Diseases*, 21(1):1–9, 2021.

- 395 [17] Fei Zhou, Ting Yu, Ronghui Du, Guohui Fan, Ying Liu, Zhibo Liu, Jie Xiang, Yeming Wang,  
396 Bin Song, Xiaoying Gu, Lulu Guan, Yuan Wei, Hui Li, Xudong Wu, Jiuyang Xu, Shengjin  
397 Tu, Yi Zhang, Hua Chen, and Bin Cao. Clinical course and risk factors for mortality of adult  
398 inpatients with covid-19 in wuhan, china: a retrospective cohort study. *Lancet*, 2020.
- 399 [18] Nithya C Achaiah, Sindhu B Subbarajasetty, and Rajesh M Shetty. R0 and re of covid-19:  
400 Can we predict when the pandemic outbreak will be contained? *Indian journal of critical*  
401 *care medicine: peer-reviewed, official publication of Indian Society of Critical Care Medicine*,  
402 24(11):1125, 2020.
- 403 [19] Matt J Keeling and Pejman Rohani. *Modeling infectious diseases in humans and animals*.  
404 Princeton university press, 2011.
- 405 [20] Micaela Morettini, Agnese Sbrollini, Ilaria Marcantoni, and Laura Burattini. Covid-19 in  
406 italy: Dataset of the italian civil protection department. *Data in brief*, 30:105526, 2020.
- 407 [21] Kenneth P Burnham and David R Anderson. Multimodel inference: understanding aic and  
408 bic in model selection. *Sociological methods & research*, 33(2):261–304, 2004.
- 409 [22] Malen Etxeberria-Etxaniz, Santiago Alonso-Quesada, and Manuel De la Sen. On an seir  
410 epidemic model with vaccination of newborns and periodic impulsive vaccination with eventual  
411 on-line adapted vaccination strategies to the varying levels of the susceptible subpopulation.  
412 *Applied Sciences*, 10(22):8296, 2020.
- 413 [23] P. van den Driessche and James Watmough. Reproduction numbers and sub-threshold en-  
414 demic equilibria for compartmental models of disease transmission. *Mathematical Biosciences*,  
415 180(1):29–48, 2002.
- 416 [24] Fred Brauer, Carlos Castillo-Chavez, and Carlos Castillo-Chavez. *Mathematical models in*  
417 *population biology and epidemiology*, volume 2. Springer, 2012.